View-Order Consideration for Hyperpolarized C-13 Imaging with Radial Acquisition and Projection Reconstruction

K. Wang[1], E. Peterson[2], J. Gordon[1], K. Kurpad[3], I. Rowland[3], M. Erickson[3], and S. Fain[1,3]
[1]Medical Physics, University of Wisconsin-Madison, Madison, WI, United States, [2]Biomedical Engineering, University of Wisconsin-Madison, Madison, WI, United States, [3]Radiology, University of Wisconsin-Madison, Madison, WI, United States

INTRODUCTION

Hyperpolarized (HP) C-13 compounds exhibit non-equilibrium T_1 decay and rapidly evolving spectral dynamics, and it is highly desirable to develop pulse sequences to image C-13 compounds in the spatial-spectral-time domain with high resolution in all dimensions. However, due to the non-equilibrium state of the non-recoverable hyperpolarized magnetization, every RF excitation for a typical GRE pulse sequence consumes a fraction of the total magnetization and therefore sets a limit on the total number of RF pulses that can be played out during the entire imaging protocol. Due to the resistance of non-Cartesian sampling methods, such as radial [1] and spiral imaging [2] to under-sampling artifacts they are very desirable for imaging hyperpolarized media. In addition, variable flip angle (VFA) [3,4] was introduced to address the issue of the intrinsic k-space modulation due to the RF induced magnetization loss. However, VFA approaches become infeasible in circumstances of B_1 in-homogeneities and therefore constant transmission power is favorable under these circumstances. In this work, we first performed simulations to investigate the impact of RF-induced k-space modulation using constant flip angle for HP C-13 2D radial imaging. Three different view order schemes were selected for comparison, and a superior scheme was found with respect to minimizing the induced spatial artifacts. An HP C-13 phantom experiment was further performed to validate the simulation results using a radial acquisition sequence.

THEORY

Due to the non-equilibrium state of hyperpolarized species, the longitudinal magnetization, Mz, is constantly decreasing due to two factors: 1. Exponential decay of the non-equilibrium polarization to thermal equilibrium state, i.e. T1 decay; and 2. previous RF excitations. If a constant flip angle is used, the magnitude of the transverse magnetization, Mxy, immediately after each RF pulse will also decrease from one TR to the next. This will cause an intrinsic modulation in the acquired raw data, i.e. a filter in k-space, resulting in blurring or other artifacts in image space [5]. Just considering the effect of the RF pulse, Mxy will obey Eq. (1), where k is the index of the RF excitation during the entire imaging protocol, and α is the flip angle.

$$M_{xy}(k) = M_0(\cos\alpha)^{k-1}\sin\alpha, k = 1,2,3... \quad (1)$$

$$RRMS = \sqrt{\frac{\sum_i \left\| I_i^{ref} - I_i^{HP} \right\|^2}{\sum_i \left\| I_i^{ref} \right\|^2}} \quad (2)$$

MATERIALS AND METHODS

First, an MR image of a proton resolution phantom was used to test the impact of the RF-induced intrinsic k-space modulation for radial imaging. Since the T_1 for HP C-13 is about 40 s and a typical scan time for acquiring a single 2D image is about 2 s, the loss of magnetization due to T_1 decay was ignored in the simulation. Three different projection order schemes were compared: sequential, golden angle ($\Delta\theta=111.25^O$) with angular weighting [6] and bit-reversal. The original image was first Radon-transformed to sinogram space, and each projection was multiplied by a weighting factor based on Eq. (1) and its location in the excitation train, mimicking HP C-13 imaging conditions. Then filtered back-projection (FBP) was used to reconstruct corresponding images. In addition, a reference image was generated by performing FBP directly on the projection data without additional weighting, simulating conventional thermal imaging condition. Simulation parameters included: matrix size = 128^2, 128 projections, and flip angles of 1^O, 5^O and 10^O were simulated. In an attempt to quantify the performance of each ordering scheme, a net error was calculated as the relative root mean squared (RRMS) error between the thermal reference and the HP image, shown by Eq. (2), as used in other work [7,8]. In order to eliminate the mean value offset caused by RF excitations, all HP images were scaled such that their mean signal intensities matched that of the reference image prior to RRMS calculation. In the HP C-13 experiment, sequential and bit-reversal schemes were compared in a small syringe containing C-13 pyruvate. Matrix size = 64^2 with 64 projections for each scheme. A surface coil was used and the average flip angle was about 8^O.

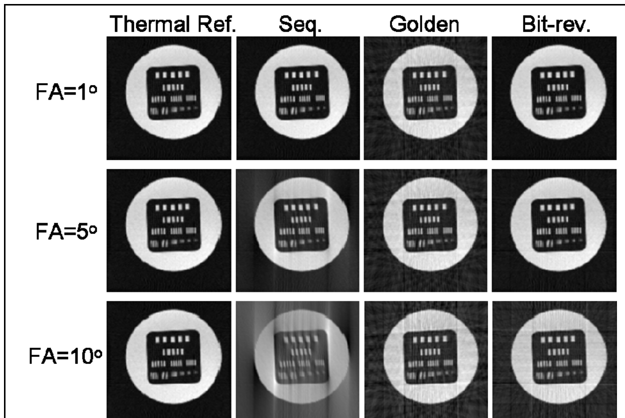

Figure 1. Comparison of three view order schemes for a range of flip angles. Bit-reversal method presents the least artifacts level for all simulated flip angles. Typical flip angles for real HP C-13 experiments are about 5^O~10^O.

Table 1. RRMS Values

	Sequential	Golden Angle	Bit-reversal
FA = 1^O	0.0042	0.052	0.00066
FA = 5^O	0.11	0.052	0.017
FA = 10^O	0.41	0.078	0.070

RESULTS

The reference image and all simulated HP images are compared in Fig. 1. For all the flip angles simulated, the bit-reversal scheme exhibits the most artifact free image, i.e. fewest streaks and signal modulations. For a 5^O flip angle, the sequential scheme shows evident streaks due to the fact that the first few projections (near 0 degree projection angle) have a higher intensity than others, resulting in dominating artifacts along the vertical direction. The golden angle scheme mitigates this artifact, but since sampled radial lines are not strictly equal-spaced, image artifacts remain even after angular density compensation (Fig. 1, 3rd column). Bit-reversal ordering can achieve both strictly equal-spaced and distributed radial lines and therefore approaches the ideal reference, in terms of SNR and image resolution. For FA=10^O, the sequential scheme is almost unusable due to the severe streaks caused by the early projections. While the golden angle and the bit-reversal schemes show the same image resolution as the reference, with tolerable image artifacts, the bit-reversal scheme is still preferable due to the strictly equal-spaced radial sampling. This observation can also be validated quantitatively by the RRMS measurements listed in Table 1. For all flip angles, bit-reversal ordering shows the smallest difference among all three schemes when compared to the reference image. These results were further validated with respect to sequential ordering in the HP C-13 experiment, shown in Fig. 2. The bit-reversal scheme shows superior image quality over the sequential method in term of streak artifact suppression.

Figure 2. Experimental comparison results for phantom containing HP C-13 urea (same window level).

DISCUSSION AND CONCLUSIONS

In this work, we investigated qualitatively and quantitatively the impact of the RF excitation-induced k-space modulation for HP C-13 imaging using radial acquisition with three different projection order strategies. It was found that at low flip angle (<8^O), radial acquisition with a bit-reversal scheme is able to preserve the image resolution with unnoticeable streak artifacts. At higher flip angle (>10^O), the bit-reversal method also shows the smallest image errors if compared to a sequential or golden angle method. In the case where a homogeneous flip angle is achievable, a variable flip angle method is expected to further improve the performance of any scheme for a wider range of flip angles. If B_1 suffers from severe inhomogeneies (e.g. the use of a surface coil) and a constant transmission power is used, a bit-reversal scheme is preferred for HP C-13 radial imaging.

ACKNOWLEDGMENTS We grateful acknowledge GE Healthcare for their assistance and NIH for funding support.
REFERENCES [1] Holmes et al., MRM 2008; 59:1062-1071 [2] Mayer et al., MRM, 2009; 62:557-564 [3] Mansfield, MRM; 1:370-386 [4] Sobering et al., ISMRM 1995; p687 [5] Yen et al., MRM 2009; 62:1-10 [6] Winkelmann et al., IEEE Trans Med Imag 2007; 26:68-76 [7] Park et al., MRM 2005; 53:186-193 [8] Brau et al., MRM 2008; 59:382-395